arXiv:astro-ph/0302357v3 2 Jul 2003

Is the present expansion of the universe really accelerating?

R G Vishwakarma

Inter-University Centre for Astronomy and Astrophysics (IUCAA),
Post Bag 4, Ganeshkhind, Pune 411 007, India
Email: vishwa@iucaa.ernet.in

Abstract

The current observations are usually explained by an accelerating expansion of the present universe. However, with the present quality of the supernovae Ia data, the allowed parameter space is wide enough to accommodate the decelerating models as well. This is shown by considering a particular example of the dark energy equation-of-state $w_\phi \equiv p_\phi/\rho_\phi = -1/3$, which is equivalent to modifying the *geometrical curvature* index k of the standard cosmology by shifting it to $(k - \alpha)$ where α is a constant. The resulting decelerating model is consistent with the recent CMB observations made by WMAP, as well as, with the high redshift supernovae Ia data including SN 1997ff at $z = 1.755$. It is also consistent with the newly discovered supernovae SN 2002dc at $z = 0.475$ and SN 2002dd at $z = 0.95$ which have a general tendency to improve the fit.

Key words: cosmology: theory, dark energy, CMB observations, SNe Ia observations.

1 INTRODUCTION

It is generally believed that the expansion of the present universe is accelerating, fuelled by some hypothetical source with negative pressure collectively known as *'dark energy'*. This belief is mainly motivated by the high redshift supernovae (SNe) Ia observations, which cannot be explained by the decelerating Einstein deSitter model which used to be the favoured model before these observations were made a few years ago. (It may, however, be noted that if one takes into account the absorption of light by the inter-galactic metallic dust which extinguishes radiation travelling over long distances, then the observed faintness of the extra-galactic SNe Ia can be explained successfully in the framework of the Einstein deSitter model. This issue will be

discussed in a later section. In the rest of the discussion, we shall not include this effect.)

Although the best-fitting standard model to the SNe Ia data predicts an accelerating expansion, however, it should be noted that the low density open models, which predict a decelerating expansion, also fit the SNe Ia observations reasonably well. Unfortunately, these models are ruled out by the recent measurements of the angular power fluctuations of CMB including the first year observations made by WMAP.

In this paper we show, by considering a particular example, that both these observations (and many others too) can still be explained by a decelerating model of the universe in the mainstream cosmology.

The observed SNe Ia explosions look fainter than their luminosity in the Einstein-deSitter model. This observed faintness is explained by invoking a positive cosmological constant Λ following the fact that the luminosity distance of an object can be increased by incorporating a *'matter'* with negative pressure in Einstein's equations. However, a constant Λ, is plagued with the so called the cosmological constant problem: Why don't we see the large vacuum energy density $\rho_{\rm v} \equiv \Lambda/8\pi G = \rho_{\rm Pl} \approx 10^{76}$ GeV^4, expected from particle physics which is $\approx 10^{123}$ times larger than the value required by the SNe observations? Or, why are the radiation energy density and the energy density in Λ ($\Lambda/8\pi G$) set to an accuracy of better than one part in 10^{123} at the Planck time in order to ensure that the densities in matter and Λ become comparable at precisely the present epoch? (Padmanabhan 2002; Peebles & Ratra 2003; Sahni & Starobinsky 2000). A phenomenological solution to understand the smallness of Λ is supplied by a dynamically decaying Λ. A popular candidate is an evolving large-scale scalar field ϕ, commonly known as *quintessence*, which does not interact with matter ($T_\phi^{ij}{}_{;j} = 0$) and can produce negative pressure for a potential energy-dominated field (Peebles & Ratra 2003). This is equivalent to generalizing the equation of state of vacuum to

$$p_\phi = w_\phi \rho_\phi. \tag{1}$$

Moreover, it is always possible to add a term like T_ϕ^{ij} on the right hand side of Einstein's field equations independent of the geometry of the universe. The equation-of-state parameter w_ϕ is, in general, some function of time and leads to a constant Λ for $w_\phi = -1$.

It would be worthwhile to mention here that there is another approach

to understand the smallness of Λ by invoking some phenomenological models of kinematical Λ which result either from some symmetry principle (Vishwakarma 2001a, 2001b), or from dimensional analysis (Vishwakarma 2000, 2002a; Carvalho, Lima & Waga 1992; Chen & Wu 1990) or just by assuming Λ as a function of the cosmic time t or the scale factor $S(t)$ of the R-W metric (for a list of this type of models, see Overduin & Cooperstock 1998). Although the quintessence fields also behave like a dynamical Λ (with $\Lambda_{\rm effective} \equiv 8\pi G\rho_\phi$), they are in general fundamentally different from the kinematical Λ models. In the former case, quintessence and matter fields are assumed to be conserved separately, whereas in the latter case, the conserved quantity is $[T^{ij}_{\rm matter} + \{\Lambda(t)/8\pi G\}g^{ij}]$, which follows from the vanishing divergence of the Einstein tensor. This characteristic of the kinematical Λ models makes them consistent with Mach's principle (Vishwakarma 2002b). However, in the following, we shall keep ourselves limited to the former case with a constant w_ϕ.

2 FIELD EQUATIONS AND DISTANCE MEASURES

In order to study the constraints on the parameters coming from the different observations, we shall describe the model briefly in the following. For the R-W metric, the Einstein field equations, taken together with conservation of the energy, yield

$$H^2(z) = H_0^2\left[\Omega_{\rm m0}\,(1+z)^3 + \Omega_{\rm r0}(1+z)^4 + \Omega_{\phi 0}(1+z)^{3(1+w_\phi)} - \Omega_{k0}\,(1+z)^2\right], \quad (2)$$

$$q(z) = \frac{H_0^2}{H^2(z)}\left[\frac{\Omega_{\rm m0}}{2}(1+z)^3 + \Omega_{\rm r0}(1+z)^4 + \frac{(1+3w_\phi)}{2}\Omega_{\phi 0}(1+z)^{3(1+w_\phi)}\right], \quad (3)$$

where Ω_i are, as usual, the different energy density components in units of the critical density $\rho_{\rm c} \equiv 3H^2/8\pi G$:

$$\Omega_{\rm m} \equiv \frac{8\pi G}{3H^2}\rho_{\rm m}, \quad \Omega_{\rm r} \equiv \frac{8\pi G}{3H^2}\rho_{\rm r}, \quad \Omega_\phi \equiv \frac{8\pi G}{3H^2}\rho_\phi, \quad \Omega_k \equiv \frac{k}{S^2H^2} \quad (4)$$

and the subscript 0 denotes the value of the quantity at the present epoch. Equation (2) at $z = 0$ implies that $\Omega_{\rm m0} + \Omega_{\rm r0} + \Omega_{\phi 0} = 1 + \Omega_{k0}$, by the use of which Equation (2) reduces to

$$H^2(z) = H_0^2 \Big[\Omega_{\rm m0}\,(1+z)^3 + \Omega_{\rm r0}(1+z)^4 + \Omega_{\phi 0}(1+z)^{3(1+w_\phi)} + (1-\Omega_{\rm m0}-\Omega_{\rm r0}-\Omega_{\phi 0})\,(1+z)^2\Big]. \quad (5)$$

In a homogeneous and isotropic universe, the different distance measures of a light source of redshift z located at a radial coordinate distance r_1 are given by the following.
The *luminosity distance* $d_{\rm L}$:

$$d_{\rm L} = (1+z) S_0\, r_1, \quad (6)$$

The *angular diameter distance* $d_{\rm A}$:

$$d_{\rm A} = \frac{S_0\, r_1}{(1+z)}, \quad (7)$$

where r_1 is given by

$$r_1 = \begin{cases} \sin\left(\frac{1}{S_0}\int_0^z \frac{{\rm d}z'}{H(z')}\right), & \text{when} \quad k=1 \\ \frac{1}{S_0}\int_0^z \frac{{\rm d}z'}{H(z')}, & \text{when} \quad k=0 \\ \sinh\left(\frac{1}{S_0}\int_0^z \frac{{\rm d}z'}{H(z')}\right), & \text{when} \quad k=-1. \end{cases} \quad (8)$$

The present value of the scale factor S_0, appearing in equations (6 - 8) which measures the curvature of spacetime, can be calculated from equation (4) as

$$S_0 = H_0^{-1}\sqrt{\frac{k}{(\Omega_{\rm m0}+\Omega_{\rm r0}+\Omega_{\phi 0}-1)}}. \quad (9)$$

3 DEGENERACIES IN FRIEDMANN MODELS COMING FROM SNe Ia OBSERVATIONS

Let us start with the SNe Ia observations which directly measure the apparent magnitude m and the redshift z of the supernovae. The theoretically predicted (apparent) magnitude $m(z)$ of a light source at a given redshift z

is given in terms of its absolute luminosity M and the luminosity distance $d_{\rm L}$ through the relation

$$m(z) = \log_{10}[\mathcal{D}_{\rm L}(z)] + \mathcal{M}, \tag{10}$$

where $\mathcal{D}_{\rm L} \equiv H_0 d_{\rm L}$ is the dimensionless luminosity distance and $\mathcal{M} \equiv M - 5\,\log_{10} H_0 +$ *constant* (the value of the *constant* depends on the chosen units in which $d_{\rm L}$ and H_0 are measured. For example, if $d_{\rm L}$ is measured in Mpc and H_0 in km s^{-1} Mpc^{-1}, then this *constant* comes out as $\approx$25).

We consider the data on the redshift and magnitude of a sample of 54 SNe Ia as considered by Perlmutter et al (excluding 6 outliers from the full sample of 60 SNe) (Perlmutter et al 1999), together with SN 1997ff at $z = 1.755$ ($m^{\rm eff} = 26.02 \pm 0.34$), the highest redshift supernova observed so far (Riess et al 2001; Narciso et al 2002). In addition to this old sample of 55 SNe, we also consider the two newly discovered supernovae SN 2002dc at $z = 0.475$ ($m^{\rm eff} = 22.73 \pm 0.23$) and SN 2002dd at $z = 0.95$ ($m^{\rm eff} = 24.68 \pm 0.2$), which have been discovered with the help of the recently installed *Advanced Camera for Surveys* on the *Hubble Space Telescope* (HST) (Blakeslee et al. 2003). In the following, we shall also keep an eye on how the addition of these SNe to the older sample affects the fit.

The χ^2 value is calculated from its usual definition

$$\chi^2 = \sum_{i=1}^{N} \left[\frac{m_i^{\rm eff} - m(z_i)}{\delta m_i^{\rm eff}} \right]^2, \tag{11}$$

where N is the number of data points (SNe) considered, $m_i^{\rm eff}$ refers to the effective magnitude of the ith SN which has been corrected for the SN lightcurve width-luminosity relation, galactic extinction and K-correction. The dispersion $\delta m_i^{\rm eff}$ is the uncertainty in $m_i^{\rm eff}$.

If one minimizes χ^2 in the standard cosmology ($w_\phi = -1$) by varying the free parameters $\Omega_{\rm m0}$, $\Omega_{\phi 0} = \Omega_{\Lambda 0}$ and $\mathcal{M}$ (the contribution from the term containing $\Omega_{\rm r0}$ is negligible for this dataset and can be safely neglected), one finds that the best-fitting solution, from the older sample of 55 SNe, is $\Omega_{\rm m0} = 0.67$, $\Omega_{\Lambda 0} = 1.24$ and $\mathcal{M} = 23.92$ with $\chi^2 = 56.93$ at 52 degrees of freedom (dof) (= number of data points $N-$ number of fitted parameters), i.e., $\chi^2/{\rm dof} = 56.93/52 = 1.09$, a good fit indeed. Addition of the new SNe to the older sample gives a similar best-fitting model: $\Omega_{\rm m0} = 0.64$,

$\Omega_{\Lambda 0} = 1.20$ and $\mathcal{M} = 23.92$ with $\chi^2/\mathrm{dof} = 57.78/54 = 1.07$, showing a slight improvement in the fit.

A *'rule of thumb'* for a *moderately* good fit is that χ^2 should be roughly equal to the number of dof. A more quantitative measure for the *goodness-of-fit* is given by the χ^2-*probability* which is very often met with in the literature and its compliment is usually known as the *significance level* (should not be confused with the confidence regions). If the fitted model provides a typical value of χ^2 as x at n dof, this probability is given by

$$Q(x,n) = \frac{1}{\Gamma(n/2)} \int_{x/2}^{\infty} e^{-u} u^{n/2-1} \mathrm{d}u. \tag{12}$$

Roughly speaking, it measures the probability that *the model does describe the data and any discrepancies are mere fluctuations which could have arisen by chance*. To be more precise, $Q(x,n)$ gives the probability that a model which does fit the data at n dof, would give a value of χ^2 as large or larger than x. If Q is very small, the apparent discrepancies are unlikely to be chance fluctuations and the model is ruled out.

The probability Q for the best-fitting standard model comes out as 29.7% (without including the new points) and 33.7% (with the new points), which represent good fits. These models represent accelerating expansion of the present universe according to equation (3), which suggests that $q_0 < 0$ if $w_\phi < -1/3$ and $\Omega_{\phi 0} > \Omega_{\mathrm{m}0}/(3 \mid w_\phi \mid -1)$. Thus the best-fitting flat model ($\Omega_\mathrm{m} + \Omega_\Lambda = 1$) is also an accelerating one, which is obtained as $\Omega_{\mathrm{m}0} = 1 - \Omega_{\Lambda 0} = 0.31$ with $\chi^2/\mathrm{dof} = 58.97/53 = 1.11$ and $Q = 26.6\%$, from the older sample of 55 SNe. Addition of the new points improves the fit marginally by giving $\Omega_{\mathrm{m}0} = 0.32$ with $\chi^2/\mathrm{dof} = 59.67/55 = 1.08$ and $Q = 31\%$, as the new best-fitting solution.

Let us now examine the status of the decelerating models, particularly, the models with $\Omega_\phi = 0$. An important model in this category is the canonical Einstein-deSitter model ($\Omega_{\mathrm{m}0} = 1$, $\Omega_{\Lambda 0} = 0$), which has a poor fit: $\chi^2/\mathrm{dof} = 93.01/54 = 1.72$ with $Q = 0.08\%$, from the older sample of 55 points. Even the addition of the new points does not improve the fit significantly, giving $\chi^2/\mathrm{dof} = 94.61/56 = 1.69$ with $Q = 0.1\%$ and the model is ruled out. However, the open models with low $\Omega_{\mathrm{m}0}$ have reasonable fits. For example, the following decelerating models with $\Lambda = 0$ (even without including the new points) provide:
$\Omega_{\mathrm{m}0} = 0.2$: $\chi^2/\mathrm{dof} = 66.74/54 = 1.24$, $Q = 11.4\%$;

$\Omega_{\rm m0} = 0.3$: $\chi^2/{\rm dof} = 68.78/54 = 1.27$, $Q = 8.5\%$;
$\Omega_{\rm m0} = 0.4$: $\chi^2/{\rm dof} = 71.31/54 = 1.32$, $Q = 5.7\%$, etc.,
which have reasonable fits and by no means are rejectable. Addition of the new points improves the fits marginally, giving:
$\Omega_{\rm m0} = 0.2$: $\chi^2/{\rm dof} = 67.04/56 = 1.2$, $Q = 14.8\%$;
$\Omega_{\rm m0} = 0.3$: $\chi^2/{\rm dof} = 69.09/56 = 1.23$, $Q = 11.2\%$;
$\Omega_{\rm m0} = 0.4$: $\chi^2/{\rm dof} = 71.69/56 = 1.28$, $Q = 7.7\%$, etc.
Open decelerating models with non-zero Λ ($0 < \Omega_{\Lambda 0} < \Omega_{\rm m0}/2$) have even better fit. The best-fitting model with a vanishing Λ is obtained as $\Omega_{\rm m0} = 0$ with $\chi^2 = 64.6$ at 54 dof ($\chi^2/{\rm dof} = 1.2$) and $Q = 15.3\%$, from the older sample of 55 points. Addition of the new points to this sample improves the fit by giving $\chi^2/{\rm dof} = 65.15/56 = 1.16$, $Q = 18.8\%$.

Figure 1 shows the allowed regions by the full data in the $\Omega_{\rm m0} - \mathcal{M}$ plane at different confidence levels for a vanishing Λ cosmology. Thus the low $\Omega_{\rm m0}$ open models with a vanishing Λ are fully consistent with the current SNe Ia observations. This result is also consistent with the findings of Gott et al (2001) from their median statistics analysis that the open models with low density and vanishing Λ are not inconsistent with the SNe Ia data. Additionally, a low $\Omega_{\rm m0}$ is also consistent with the recent 2DF and Sloan surveys which give $\Omega_{\rm m0} = 0.23 \pm 0.09$ (Hawkins et al. 2002) and $\Omega_{\rm m0} \approx 0.14^{+0.11}_{-0.06}$ (at 2σ) (Dodelson et al. 2001). However, these models do not seem consistent with the first-year observations of the temperature angular power spectrum of the CMB, measured accurately by NASA's explorer mission "Wilkinson Microwave Anisotropy Probe" (WMAP) (Bennett et al., 2003), or even with the earlier CMB observations (de Bernardis et al. 2000, 2002; Lee et al. 2001; Halverson et al. 2002; Siever et al. 2002). These observations, when fitted to the standard cosmology, appear to indicate that $\Omega_{\rm m0} + \Omega_{\Lambda 0} \approx 1$.

4 THE PROPOSED MODEL

4.1 Motivation

We shall now consider a particular model of dark energy specified by the equation of state $w_\phi = -1/3$, which, as we shall show in the following, explains both the observations - SNe Ia, as well as, CMB - very well. The equation of state $w_\phi = -1/3$, for which ρ_ϕ varies as $1/S^2$ (say, $\Omega_\phi = \alpha/S^2H^2$), is interesting in its own right. For this case, the Hubble and the deceleration

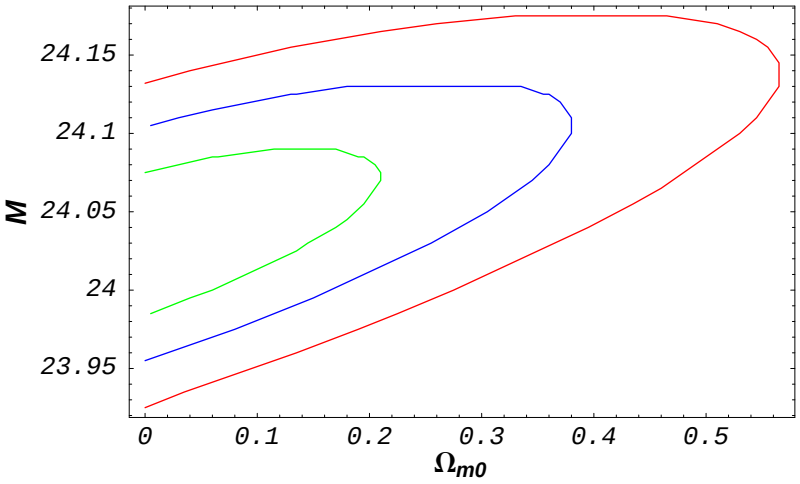


Figure 1: The allowed regions by the SNe Ia data (with 57 points) are shown in the $\Omega_{\rm m0} - \mathcal{M}$ plane for $\Omega_\phi = 0$ cosmology ($\mathcal{M}$ is usually termed as the '*Hubble constant-free absolute luminosity*'). The ellipses, in the order of increasing size, correspond to respectively 68%, 95% and 99% confidence levels.

parameters reduce respectively to

$$H^2(z) = H_0^2 \left[\Omega_{\rm m0}\,(1+z)^3 + \Omega_{\rm r0}(1+z)^4 + (1-\Omega_{\rm m0}-\Omega_{\rm r0})\,(1+z)^2\right], \quad (13)$$

$$q(z) = \frac{H_0^2}{H^2(z)}\left[\frac{\Omega_{\rm m0}}{2}(1+z)^3 + \Omega_{\rm r0}(1+z)^4\right], \quad (14)$$

which describe a decelerating expansion. Interestingly in this case, $\Omega_{\rm matter}$ ($\equiv \Omega_{\rm m} + \Omega_{\rm r}$) alone is sufficient to describe $H(z)$ completely, which gives the expansion dynamics of the universe. The additional knowledge of $\Omega_{\phi 0}$ decides the curvature through $\Omega_{k0} = \Omega_{\rm m0} + \Omega_{\rm r0} + \Omega_{\phi 0} - 1$. Expressions (13) and (14) are the same as the ones in the standard cosmology with $\Lambda = 0$, with only one exception: in the standard cosmology, $\Omega_{\rm m0} + \Omega_{\rm r0} = 1 + \Omega_{k0}$, whereas in the present model, $\Omega_{\rm m0} + \Omega_{\rm r0} + \Omega_{\phi 0} = 1 + \Omega_{k0}$. As mentioned earlier, $\Omega_{\phi 0}$ contributes to the curvature through $S_0 = H_0^{-1}\sqrt{k/(\Omega_{\rm m0} + \Omega_{\rm r0} + \Omega_{\phi 0} - 1)}$

and hence to the different distance measures for $k = \pm 1$ cases (for $k = 0$, distances do not depend on S_0). Although $\Omega_{\phi 0}$ does not contribute to the expansion dynamics of the model (and neither to the distances for $k = 0$ case), it helps $\Omega_{\rm m0}$ to assume even those values which are not allowed in the standard cosmology, and hence gives more leverage to $\Omega_{\rm m0}$. It is in fact this property of the model which is instrumental in explaining the CMB observations even for low $\Omega_{\rm m0}$, as we shall see in the following.

It may be noted that although the topological defects, like cosmic strings and textures, also have an equation of state $\rho + 3p = 0$ (i.e., their density falls off as $1/S^2$), however, the converse of this is not true and a dark energy with $w_\phi = -1/3$ need not necessarily be represented by cosmic strings. Moreover, this 'pseudo-source' term does not explicitly contribute to the expansion dynamics (and hence to the deceleration or to the expansion age) of the model but essentially to the curvature, as we have mentioned earlier. One can obtain the same cosmology by removing this term and simultaneously modifying the curvature index k by $(k - \alpha)$ (Vishwakarma & Singh 2002). It would, therefore, be more appropriate to consider it as a shift in the *geometrical curvature* of the standard cosmology and not as a source term. This term also appears in the context of brane cosmology by adding a surface term of brane curvature scalar in the action (Vishwakarma & Singh 2003; Singh, Vishwakarma & Dadhich 2002).

4.2 CMB Observations

The temperature fluctuations ΔT in the angular power spectra of the CMB correspond to oscillations in the ΔT - ℓ (Legendre multipole) space. The peaks of these oscillations can be explained in terms of the angle $\theta_{\rm A}$ subtended by the sound horizon at the last scattering epoch when CMB photons decoupled from baryons at $z_{\rm dec} = 1100$ (Hu & Dodelson 2002). The power spectrum of CMB can be characterized by the positions of the peaks and ratios of the peak amplitudes. It has long been recognized that the locations and amplitudes of the peaks in the region $90 < \ell < 900$ (where the anisotropies are related to causal processes occurring in the photon-baryon plasma until recombination) are very sensitive to the variations in the parameters of the model and hence serve as a sensitive probe to constrain the cosmological parameters and discriminate among various models (Hu et al. 2001; Doran & Lilley 2001, 2002). In fact, for $\ell > 40$, the ratios of the peak amplitudes are insensitive to the intrinsic amplitude of the CMB spectrum.

This renders the positions of the peaks, particularly the position of the first peak, as a powerful probe of the parameters of the model. The first-year observations of WMAP have measured the position of the first peak very accurately at $\ell = 220.1 \pm 0.8$ (1 σ) (Page et al. 2003), which we shall use in our fit.

The angle $\theta_{\rm A}$, which is given by the ratio of sound horizon to the distance (*angular diameter distance*) of the last scattering surface, sets the acoustic scale $\ell_{\rm A}$ through

$$\ell_{\rm A} = \frac{\pi}{\theta_{\rm A}} = \frac{\pi\ S_0\ r_1(z_{\rm dec})}{\int_{z_{\rm dec}}^{\infty} c_{\rm s}(z)\ {\rm d}z/H(z)}, \tag{15}$$

where the speed of sound $c_{\rm s}$ in the plasma is given by $c_{\rm s} = 1/\sqrt{3(1+R)}$ and $R \equiv 3\rho_{\rm b}/4\rho_\gamma = 3\Omega_{\rm b0}/[4\Omega_{\gamma 0}(1+z)]$ corresponds to the ratio of baryon density to photon density. The location of i-th peak in the angular power spectrum is given by

$$\ell_{\rm peak_i} = \ell_{\rm A}(i - \delta_i), \tag{16}$$

where the phase shift δ_i, caused by the plasma driving effect, is determined predominantly by the pre-recombination physics (Hu et al. 2001) and can be approximated by

$$\delta_i = a_i \left\{ \frac{\Omega_{\rm r0}(1+z_{\rm dec})}{0.3\ \Omega_{\rm m0}} \right\}^{0.1}, \tag{17}$$

where a_i is respectively 0.267, 0.24 and 0.35 for peak$_1$, peak$_2$ and peak$_3$. Let us recall that $\Omega_{\rm r0}$ gets contributions from photons (CMB) as well as from neutrinos, i.e., $\Omega_{\rm r} = \Omega_\gamma + \Omega_\nu$. The present photon contribution to the radiation can be estimated from the CMB temperature $T_0 = 2.728$K. This gives $\Omega_{\gamma 0} \approx 2.48\ h^{-2} \times 10^{-5}$, where h is the present value of the Hubble parameter in units of 100 km s^{-1} Mpc^{-1}. The neutrino contribution follows from the assumption of 3 neutrino species, a standard thermal history and a negligible mass compared to its temperature (Hu & Dodelson 2002) leading to $\Omega_{\nu 0} \approx 1.7\ h^{-2} \times 10^{-5}$.

Equations (15)-(17), suplimented by (8) and (9), are now fully capable to compute the locations of the peaks for given values of the free parameters $\Omega_{\rm m0}$, $\Omega_{\phi 0}$, $\Omega_{\rm b0}$ and h. We notice that a sufficiently big range of these parameters produce the $\ell_{\rm peak_i}$ values in the observed range. For example, by fixing $\Omega_{\rm b0} = 0.05$ and $h = 0.65$, the following choices of $\Omega_{\rm m0}$ and $\Omega_{\phi 0}$ yield:

$\Omega_{\rm m0} = 0.3$, $\Omega_{\phi 0} = 0.6 \rightarrow \ell_{\rm peak_1} = 222.5$, $\ell_{\rm peak_2} = 536.7$, $\ell_{\rm peak_3} = 808.2$;

$\Omega_{\rm m0} = 0.25$, $\Omega_{\phi 0} = 0.65 \rightarrow \ell_{\rm peak_1} = 225.0$, $\ell_{\rm peak_2} = 545.1$, $\ell_{\rm peak_3} = 820.9$;

$\Omega_{\rm m0} = 0.2$, $\Omega_{\phi 0} = 0.72 \rightarrow \ell_{\rm peak_1} = 220.0$, $\ell_{\rm peak_2} = 540.7$, $\ell_{\rm peak_3} = 814.3$,

which are in reasonable agreement[1] with $\ell_{\rm peak_1} = 220.1 \pm 0.8$ and $\ell_{\rm peak_2} = 546 \pm 10$ measured by WMAP. These measurements are also consistent with other observations; for example, the BOOMERANG project (de Bernardis et al., 2002) measured the first three peaks in the ranges:
$\ell_{\rm peak_1} : 200 - 223$, $\ell_{\rm peak_2} : 509 - 561$, $\ell_{\rm peak_3} : 820 - 857$ at 68% confidence level; and
$\ell_{\rm peak_1} : 183 - 223$, $\ell_{\rm peak_2} : 445 - 578$, $\ell_{\rm peak_3} : 750 - 879$ at 95% confidence level, which are also in agreement with many other observations like, MAXIMA, DASI, CBI, etc., at least on the location of the first peak (Lee et al. 2001; Halverson et al. 2002; Sievers et al. 2002).

In Figure 2, we have shown the allowed region in the $\Omega_{\rm m0} - \Omega_{\phi 0}$ plane which produces the first peak $\ell_{\rm peak_1} = 220.1 \pm 0.8$ (68% confidence level). The marginalization over the other parameters $\Omega_{\rm b0}$ and h is achived by taking projection of the full 4-dimensional region on the $\Omega_{\rm m0} - \Omega_{\phi 0}$ plane (Press et al 1986).

It may be noted that the WMAP results obtained by Spergel et al.(2003)- that only $w_\phi < -0.78$ can be accommodated within 95% confidence regions - comes from a lot of assumptions, some of which are not consistent with many observations. For example, there are several observations which also measure smaller values of H_0, apart from the higher values (see section 4.4). However, this degeneracy has not been taken into account and they consider only that HST observation which gives $H_0 = 0.72 \pm 3({\rm stat}) \pm 7({\rm systematic})$ km s^{-1} Mpc^{-1} (Friedman et al. 2001) close to their best fit value. Note that there is also another HST Key Project which gives $H_0 = 64^{+8}_{-6}$ km s^{-1} Mpc^{-1} (Saurabh et al. 1999). Sandage and his collaborators find a value even as low as $H_0 = 58 \pm 6$ km s^{-1} Mpc^{-1} from an analysis of SNe Ia distances (Parodi et al. 2000). In Figure 2, we have instead considered all those possible combinations of the parameters $\Omega_{\rm m0} \in [0 - 1]$, $\Omega_{\phi 0} \in [0 - 1.5]$, $\Omega_{\rm b0} \in [0 - 0.1]$ and $h \in [0.5 - 0.8$, which produce $\ell_{\rm peak_1} = 220.1 \pm 0.8$. This

[1]One can have even better fit by adjusting the parameters finely. For example, one can have
$\Omega_{\rm m0} = 0.3$, $\Omega_{\phi 0} = 0.61 \rightarrow \ell_{\rm peak_1} = 219.8$, $\ell_{\rm peak_2} = 530.2$, $\ell_{\rm peak_3} = 798.4$;
$\Omega_{\rm m0} = 0.25$, $\Omega_{\phi 0} = 0.666 \rightarrow \ell_{\rm peak_1} = 220.3$, $\ell_{\rm peak_2} = 533.6$, $\ell_{\rm peak_3} = 803.5$;
with the same $\Omega_{\rm b0}$ and h.

amounts to a range of $\Omega_{\rm b0}h^2$ as $[0-0.06]$ which safely contains the range $0.01 \leq \Omega_{\rm b0}h^2 \leq 0.04$ which one essentially requires to explain the observed abundances of helium, deuterium and lithium (Narlikar & Padmanabhan 2001). It should also be noted that the most favoured values like $\Omega_{\rm m0} \approx 0.25$ and $\Omega_{\rm b0}h^2 \approx 0.02$ (or $\Omega_{\rm b0} \approx 0.05$) are compatible with a moderate $h \approx 0.65$ in this model, as we have shown in our examples.

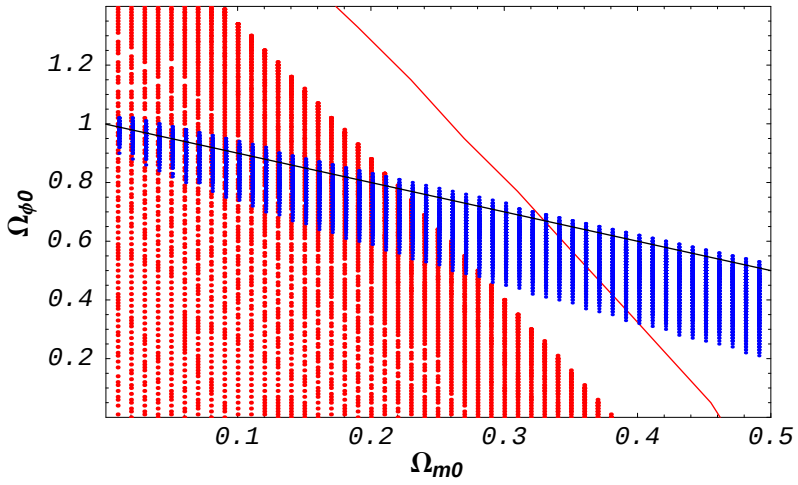


Figure 2: The blue region shows the allowed ranges of $\Omega_{\rm m0}$ and $\Omega_{\phi 0}$ by the WMAP which produce the first peak in the range 220.1 ± 0.8. This has been obtained after marginalizing over $\Omega_{\rm b0}$ and h (which have been varied in the ranges $[0-0.1]$ and $[0.5-0.8]$ respectively). The red-shaded contour corresponds to 95% confidence region (marginalized over $\mathcal{M}$) from the SNe Ia data (with all 57 points, including the two newly discovered points SN 2002dc and SN 2002dd) and the red curve corresponds to the boundary of the 99% confidence region given by the same data (in calculating these regions, the extinction of SNe light by metallic whiskers, as discussed in section 5, has *not* been taken into account). The line in black corresponds to the flat model $\Omega_{\rm m0} + \Omega_{\phi 0} = 1$.

4.3 SNe Ia Observations

For the SNe Ia data in the present model, χ^2 decreases for lower values of $\Omega_{\rm m0}$ and gives the minimum χ^2 for negative $\Omega_{\rm m0}$. For example, for the flat model, the minimum value of χ^2 is obtained as 62.93 for $\Omega_{\rm m0} = -0.31$ at 53 dof (from the older sample of 55 SNe) and 63.47 for $\Omega_{\rm m0} = -0.30$ at 55 dof (with the addition of the new points), which are though not physical. A 'physically viable' best-fitting solution, in this case, can be regarded as $\Omega_{\rm m0} = 0$, which gives $\chi^2/{\rm dof} = 64.56/53 = 1.22$ for $\Omega_{\phi 0} = 0.14$ and $\mathcal{M} = 24.03$ with $Q = 13.3\%$, from the older sample, which represents a reasonably good fit, though not as good as the best fit in the standard cosmology with a constant Λ. Moreover, the addition of the new points to this sample improves the fit, giving $\chi^2/{\rm dof} = 65.02/55 = 1.18$ for $\Omega_{\phi 0} = 0.23$ and $\mathcal{M} = 24.04$ with $Q = 16.7\%$, as the new best-fitting solution.

The allowed region by the data is sufficiently large, as shown in Figure 2, and low density models, which are also consistent with the WMAP observation, are easily accommodated within the 95% confidence region (Note that the plotted allowed region by WMAP is only at 1σ level. At higher levels, the region will be wider). For example, the following models represent reasonable fit.
$\Omega_{\rm m0} = 0.3$, $\Omega_{\phi 0} = 0.6$: $\chi^2/{\rm dof} = 71.93/54 = 1.33$ with $Q = 5.2\%$;
$\Omega_{\rm m0} = 0.25 = 1 - \Omega_{\phi 0}$: $\chi^2/{\rm dof} = 71.36/54 = 1.32$ with $Q = 5.7\%$;
$\Omega_{\rm m0} = 0.25$, $\Omega_{\phi 0} = 0.65$: $\chi^2/{\rm dof} = 70.76/54 = 1.31$ with $Q =6.3\%$;
$\Omega_{\rm m0} = 0.2$, $\Omega_{\phi 0} = 0.7$: $\chi^2/{\rm dof} = 69.63/54 = 1.29$ with $Q = 7.5\%$, etc., which are obtained from the older sample of 55 SNe. Addition of the new points improves the fits, giving:
$\Omega_{\rm m0} = 0.3$, $\Omega_{\phi 0} = 0.6$: $\chi^2/{\rm dof} = 72.44/56 = 1.29$ with $Q = 6.9\%$;
$\Omega_{\rm m0} = 0.25 = 1 - \Omega_{\phi 0}$: $\chi^2/{\rm dof} = 71.87/56 = 1.28$ with $Q = 7.5\%$;
$\Omega_{\rm m0} = 0.25$, $\Omega_{\phi 0} = 0.65$: $\chi^2/{\rm dof} = 71.22/56 = 1.27$ with $Q =8.3\%$;
$\Omega_{\rm m0} = 0.2$, $\Omega_{\phi 0} = 0.7$: $\chi^2/{\rm dof} = 70.06/56 = 1.25$ with $Q = 9.8\%$, etc.
One can go up to even as high as $\Omega_{\rm m0} \approx 0.4$ at 99% confidence level.

4.4 Age of the Universe

The parameters H_0 and $\Omega_{\rm m0}$ set the age of the universe in this model. Remember that there is still quite large uncertainty in the present value of H_0. Sandage and his collaborators find $H_0 = 58 \pm 6$ km s^{-1} Mpc^{-1} from an analysis of SNe Ia distances (Parodi et al. 2000). This is also consistent with the value obtained from an analysis of clusters using Sunyaev-Zeldovich effect

which gives $H_0 = 60 \pm 10$ km s^{-1} Mpc^{-1} (Birkinshaw 1999). An HST Key Project supplies $H_0 = 64^{+8}_{-6}$ km s^{-1} Mpc^{-1} (Saurabh et al. 1999). Some experiments also measure higher H_0, for example, another HST Key Project, which uses Cepheids to calibrate several different secondary distance indicators, finds $H_0 = 72 \pm 3$(stat)± 7(systematic) km s^{-1} Mpc^{-1} (Friedman et al. 2001). Also by using the fluctuations in the surface brightness of galaxies as distance measure, it has been found that $H_0 = 74 \pm 4$ km s^{-1} Mpc^{-1} (Blakeslee et al. 1999). Thus it appears that H_0 lies somewhere in the range $(50 - 78)$ km s^{-1} Mpc^{-1}. An average value of $H_0 = 65$ km s^{-1} Mpc^{-1} from this range, constrains $\Omega_{\rm m0}$ of the model by $0 < \Omega_{\rm m0} \leq 0.34$ to give the age of the universe $t_0 \geq 12$ Gyr, so that the age of the oldest objects detected so far, e.g., the globular clusters of age $t_{\rm GC} = 12.5 \pm 1.2$ Gyr (Cayrel et al. 2001; Gnedin et al. 2001), can be explained. The presently favoured value $\Omega_{\rm m0} \approx 0.25$ easily accommodates in this range. It is interesting to note that the average value of $H_0 = 65$ km s^{-1} Mpc^{-1} we have preferred, is in good agreement with $H_0 = 67 \pm 2$(stat)± 5(systematic) km s^{-1} Mpc^{-1} obtained recently by Gott et al (2001) from an analysis based on the median statistics.

5 EXTINCTION BY METALLIC DUST

In this section, we shall discuss the absorption of light by metallic dust ejected from the SNe explosions − an issue which is generally avoided while discussing m-z relation for SNe Ia. Although a number of observers believe this to be not a significant effect (see, for example, Riess et al (2001)), however, taking this effect into consideration does improve the fit to the data, as we shall see in the following.

It is well known that the metallic vapours are ejected from the SNe explosions which are subsequently pushed out of the galaxy through pressure of shock waves (Hoyle & Wickramasinghe, 1988; Narlikar et al, 1997). Experiments show that metallic vapours on cooling, condense into elongated whiskers of $\approx 0.5 - 1$ mm length and $\approx 10^{-6}$ cm cross-sectional radius (Hoyle et al, 2000). Indeed this type of dust extinguishes radiation travelling over long distances (Aguire, 1999; Vishwakarma, 2002a). The density of the dust can be estimated along the lines of Hoyle et al (2000). If the metallic whisker production is taken as 0.1 $M_\odot$ per SN and if the SN production rate is taken as 1 per 30 years per galaxy, the total production per galaxy (of spatial density ≈ 1 per 10^{75} cm^3) in 10^{10} years is $\approx 2/3 \times 10^{41}$ g. The expected whisker

density, hence, becomes $2/3 \times 10^{41} \times 10^{-75} \approx 10^{-34}$ g cm^{-3}. We shall later see that this value is in striking agreement with the best-fitting value coming from the SNe Ia data.

In an isotropic and homogeneous universe, the contribution to the effective magnitude arising from the absorption of light by the intervening whisker-like dust, is given by

$$\Delta m(z) = \int_0^{l(z)} \kappa \rho_g \mathrm{d}l = \kappa \rho_{g0} \int_0^z (1+z')^2 \frac{\mathrm{d}z'}{H(z')}, \tag{18}$$

where κ is the mass absorption coefficient, which is effectively constant over a wide range of wavelengths and is of the order 10^5 cm^2 g^{-1} (Wickramasinghe & Wallis, 1996), $\rho_g \propto S^{-3}$ is the whisker grain density and $l(z)$ is the proper distance traversed by light through the inter-galactic medium emitted at the epoch of redshift z. The net magnitude is then given by

$$m^{\mathrm{net}}(z) = m(z) + \Delta m(z), \tag{19}$$

where the first term on the r.h.s. corresponds to the usual magnitude from the cosmological evolution given by equation (10).

We note that taking account of this effect improves the fit to the SNe Ia data considerably. For example, the model with $\Omega_{\mathrm{m0}} = 0.25$, $\Omega_{\phi 0} = 0.65$ now gives $\chi^2/\mathrm{dof} = 65.25/53 = 1.23$ for $\mathcal{M} = 24.03$ and $\rho_{g0} = 2.02 \times 10^{-34}$ g cm^{-3} with $Q = 12.1\%$, from the older sample of 55 points. The addition of the new points improves the fit further by giving $\chi^2/\mathrm{dof} = 65.75/55 = 1.20$ for $\mathcal{M} = 24.03$ and $\rho_{g0} = 1.89 \times 10^{-34}$ g cm^{-3} with $Q = 15.2\%$. Even the Einstein-deSitter model ($\Omega_{\mathrm{m0}} = 1$, $\Omega_{\phi 0} = 0$) gives an acceptable fit: $\chi^2/\mathrm{dof} = 68.40/53 = 1.29$ for $\mathcal{M} = 24.04$ and $\rho_{g0} = 4.95 \times 10^{-34}$ g cm^{-3} with $Q = 7.6\%$ (from the 55 points-data) and $\chi^2/\mathrm{dof} = 68.97/55 = 1.25$ for $\mathcal{M} = 24.04$ and $\rho_{g0} = 4.75 \times 10^{-34}$ g cm^{-3} with $Q = 9.8\%$ (by adding the new points). Interestingly, this model (Einstein-deSitter) is also consistent with the CMB observations: $\Omega_{\mathrm{b0}} = 0.05$ and $h = 0.65$ yield $\ell_{\mathrm{peak}_1} = 202.9$, $\ell_{\mathrm{peak}_2} = 476.8$, $\ell_{\mathrm{peak}_3} = 717.6$. One can improve the fit by increasing Ω_{b0} and/or decreasing h: $\Omega_{\mathrm{b0}} = 0.1$ and $h = 0.55$ yield $\ell_{\mathrm{peak}_1} = 220.4$, $\ell_{\mathrm{peak}_2} = 521.4$, $\ell_{\mathrm{peak}_3} = 784.9$. Also a better fit can be obtained in open models. For example, the model $\Omega_{\mathrm{m0}} = 0.87$, $\Omega_{\phi 0} = 0$ with $\Omega_{\mathrm{b0}} = 0.05$ and $h = 0.65$ yields $\ell_{\mathrm{peak}_1} = 220.1$, $\ell_{\mathrm{peak}_2} = 518.8$, $\ell_{\mathrm{peak}_3} = 780.9$. This model also has an acceptable fit to the SNe Ia data: $\chi^2/\mathrm{dof} = 67.89/53 = 1.28$ for $\mathcal{M} = 24.04$

and $\rho_{g0} = 4.34 \times 10^{-34}$ g cm^{-3} with $Q = 8.2\%$ (from the 55 points-data) and $\chi^2/\mathrm{dof} = 68.45/55 = 1.24$ for $\mathcal{M} = 24.04$ and $\rho_{g0} = 4.15 \times 10^{-34}$ g cm^{-3} with $Q = 10.5\%$ (by adding the new points). However, these models suffer from the age problem if h is not sufficiently low. For example, h should be ≤ 54 for $\Omega_{\mathrm{m0}} = 1$ with $\Omega_{\phi 0} = 0$. Additionally, there is much evidence for low Ω_{m0}, as reviewed by Peebles & Ratra (2003).

6 CONCLUSION

There seems to be an impression in the community that the current observations, particularly the high redshift SNe Ia observations and the measurements of the angular power fluctuations of the CMB, can be explained only in the framework of an accelerating universe. This, however, does not seem correct. The allowed parameter space by the datasets is wide enough to accommodate decelerating models also. We have shown that both these observations can also be explained in a decelerating low density-model with a dark energy equation-of-state $w_\phi = -1/3$ and the preferred curvature of the spatial section is slightly negative. For this equation of state, the resulting 'dark energy' does not contribute to the expansion dynamics of the model (described by the Hubble parameter) and contributes to the curvature only.

In order to fit the model to the data, we have considered the most recent observations. For example, for the SNe data, we have considered the older sample of 55 SNe of type Ia (54 SNe used by Perlmutter et al + SN 1997ff at $z = 1.755$) together with the two newly discovered supernovae SN 2002dc at $z = 0.475$ and SN 2002dd at $z = 0.95$. Addition of these new points to the older sample improves the fit to, more or less, all the models. For CMB, we have considered the first-year observations of WMAP which have measured the position of the first peak very accurately.

It may be noted that the case $w_\phi = -1/3$ is not special in any sense to the datasets and slightly more decelerating or slightly less decelerating models are also consistent with both the observations. In order to verify this, we change w_ϕ slightly from $w_\phi = -1/3$ (in both directions) to, say, $w_\phi = -0.3$ and $w_\phi = -0.35$ and check the status of the resulting models. The result is the following.

$w_\phi = -0.3$:
A test model, for example, $\Omega_{\mathrm{m0}} = 0.25$, $\Omega_{\phi 0} = 0.65$, $\Omega_{\mathrm{b0}} = 0.05$ and $h = 0.65$ yields $\ell_{\mathrm{peak}_1} = 220.2$, $\ell_{\mathrm{peak}_2} = 533.4$, $\ell_{\mathrm{peak}_3} = 803.2$. The SNe Ia data, for the same model, give $\chi^2/\mathrm{dof} = 72.10/54 = 1.34$ with $Q = 5.0\%$, from the older

sample of 55 points and $\chi^2/\mathrm{dof} = 72.60/56 = 1.30$ with $Q = 6.7\%$, by adding the new points to this sample.

$w_\phi = -0.35$:
The same test model, in this case, yields $\ell_{\mathrm{peak}_1} = 227.3$, $\ell_{\mathrm{peak}_2} = 550.5$, $\ell_{\mathrm{peak}_3} = 829.1$. The SNe Ia data, for this case, give $\chi^2/\mathrm{dof} = 70.12/54 = 1.3$ with $Q = 6.9\%$, from the older sample of 55 points and $\chi^2/\mathrm{dof} = 72.57/56 = 1.26$ with $Q = 9.1\%$, by adding the new points to this sample. These fits are acceptable and comparable to their respective values for $w_\phi = -1/3$ mentioned in sections 4.2 and 4.3.

We also note that if we take into account the extinction of SNe light by the inter-galactic metallic dust, then the observed dimming of the high redshift SNe Ia can also be explained by the models without any dark energy, such as, the Einstein-deSitter model. These models are also consistent with CMB observations. In fact, there is a degeneracy in the $\Omega_{\mathrm{m}0} - \Omega_{\phi 0}$ plane along a line $\Omega_{\mathrm{m}0} + \Omega_{\phi 0} \approx 1$ and a wide range of $\Omega_{\mathrm{m}0}$ is consistent with the WMAP observation.

Interestingly, another alternative explanation of the observed faintness of SNe Ia at large distances can be given in terms of a quantum mechanical oscillation between the photon field and a hypothetical axion field in the presence of extra-galactic magnetic fields. To satisfy other cosmological constraints, one then simply needs some form of uniform dark energy with $w_\phi \approx -1/3$ and the universe would be decelerating (Csaki et al. 2002).

We conclude that it is premature to claim, on the basis of the existing data, that the present expansion of the universe is accelerating (or decelerating). Only more accurate SNe Ia data with z significantly > 1 can remove this ambiguity, as q is sensitive significantly to the SNe Ia data only. Whereas the CMB observations are consistent with both - accelerating as well as decelerating models, as mentioned above. This endeavour may be accomplished by the proposed *SuperNova Acceleration Probe* (SNAP) experiment which aims to give accurate luminosity distances of type Ia SNe up to $z \approx 1.7$.

ACKNOWLEDGEMENTS
The author thanks DAE for his Homi Bhabha postdoctoral fellowship and T. Padmanabhan for useful comments and discussions.

REFERENCES
Aguire A. N., 1999, ApJ, 512, L19

Bennett et al., astro-ph/0302207
de Bernardis P., et al., 2002, ApJ., 564, 559
Blakeslee J. P., et al., 1999, ApJ. Lett., 527, 73
Blakeslee J. P., et al., astro-ph/0302402
Birkinshaw M., 1999, Phys. Rep., 310, 97
Cayrel R., et al, 2001, Nature, 409, 691
Carvalho J. C., Lima J. A. S., Waga I., 1992, Phys. Rev. D, 46, 2404
Chen W., Wu Y. S., 1990, Phys. Rev. D, 41, 695
Csaki C., Kaloper N., Terning J., 2002, Phys. Rev. Lett., 88, 161302
Dodelson S., et al., astro-ph/0107421
Doran M., Lilley M., Schwindt J., Wetterich C., 2001, ApJ., 559, 501
Doran M., Lilley M., 2002, MNRAS, 330, 965
Freedman W. L. et al., 2001, ApJ., 553, 47
Gnedin O. Y., Lahav O., Rees M. J., astro-ph/0108034
Gott III J. R., Vogeley M. S., Podariu S., Ratra B., 2001, ApJ, 549, 1
Halverson N. W. et al., 2002, ApJ., 568, 38
Hawkins E., et al., astro-ph/0212375
Hoyle F., Wickramasinghe N. C., 1988, Astrophys. Space Sc. 147, 245
Hoyle F., Burbidge G., Narlikar J. V., 2000, *A Different Approach to Cosmology*, (Cambridge: Cambridge Univ. Press)
Hu W., Dodelson S., 2003, Ann. Rev. Astron. Astrophys., 40, 171
Hu W., Fukugita M., Zaldarriaga M., Tegmark M., 2001, ApJ., 549, 669
Lee A. T. et al., 2001, ApJ., 561, L1
Narciso B., et al., 2002, ApJ., 577, L1 (astro-ph/0207097)
Narlikar J. V., Wickramasinghe N. C., Sachs R., Hoyle F., 1997, Int. J. Mod. Phys. D, 6, 125
Narlikar J. V., Padmanabhan T., 2001, Annu. Rev. Astron. Astrophys., 39, 211
Overduin J. M., Cooperstock F. I., 1998, Phys. Rev. D, 58, 043506
Padmanabhan T., hep-th/0212290
Page et al., astro-ph/0302220
Parodi B. R., et al., 2000, ApJ., 540, 634
Peebles P. J. E., Ratra B., 2003, Rev. Mod. Phys., 75, 559 (astr0-ph/0207347)
Perlmutter S., et al., 1999, ApJ., 517, 565
Press W. H., Teukolsky S. A., Vetterling W. T., Flannery B. P., 1986, *Numerical Recipes*, (Cambridge University Press)
Riess A. G., et al., 2001, ApJ., 560, 49

Sahni V., Starobinsky A., 2000, Int. J. Mod. Phys. D 9, 373
Saurabh J., et al., 1999, ApJ. Suppl., 125, 73
Sievers J. L. et al., astro-ph/0205387
Singh P., Vishwakarma R. G., Dadhich N., hep-th/0206193
Spergel D. N. et al., astro-ph/0302209
Vishwakarma R. G., 2000, Class. Quantum Grav., 17, 3833
Vishwakarma R. G., 2001a, Gen. Relativ. Grav., 33, 1973
Vishwakarma R. G., 2001b, Class. Quantum Grav., 18, 1159
Vishwakarma R. G., 2002a, MNRAS, 331, 776
Vishwakarma R. G., 2002b, Class. Quantum Grav., 19, 4747
Vishwakarma R. G., Singh P., 2003, Class. Quantum Grav., 20, 2033
Wickramasinghe N. C., Wallis D. H., 1996, Astrophys. Space Sc. 240, 157